13th World Conference on Earthquake Engineering
Vancouver, B.C., Canada
August 1-6, 2004
Paper No. 3021

PSEUDO-DYNAMIC SEISMIC RESPONSE OF INFILLED RC FRAMES DESIGNED FOR GRAVITY LOADING

Felice COLANGELO[1]

SUMMARY

Great attention has been recently paid to the seismic assessment of those structures not designed against any seismic action. Experimental results referring to single-story single-bay half-scale reinforced-concrete frames, and deriving from in-plane pseudo-dynamic tests, are presented. Two specimens are tested bare, and five infilled by perforated-brick and mortar masonry. Frames differ as concerns their aspect ratio and reinforcement, as deformed and round bars are alternatively used. Specimens are subjected to a same natural accelerogram twice: firstly virgin, and secondly damaged owing to the previous test. Both global response and local deformation in the frame is analyzed laying emphasis on infills' effect.

INTRODUCTION

An issue currently exciting a great interest in Europe and elsewhere is the seismic assessment of those structures lacking in ductility or, from a different point of view, strength, or even both. In fact, a number of buildings designed and constructed in the absence of any seismic code are presently in use, though they are liable to a significant seismic risk in reality. In such situation, one would expect non-structural infills used for enclosing and partitioning to compensate, at least in part, for the structure deficiency.

Unfortunately, inherent fragility and concurrent failure mechanisms, where capacity design criteria were not adopted, make numeric analysis of the existing structures themselves quite difficult. An additional complication exists in that possible failure modes of the infill are to be properly identified, and coupled with those the bare structure would exhibit on its own. The out-of-plane expulsion of infills may also occur, which obviously would completely suppress their effect. Lastly, as non-structural masonry infills are of concern, variety of used materials and constructing techniques as well, applied to both the infill and its interface with the surrounding frame, is great.

Therefore, a predictive model to a reasonable degree complete, simple, and accurate, is currently pending. Seismic analysis of infilled framed structures, especially those designed for gravity load only, cannot rely on numerical simulation alone. Indeed, experimental investigation is still needed in order to support numeric analysis. This is the main objective of the present study.

[1] Associate Professor, DISAT Dept., University of L'Aquila, L'Aquila, Italy. Email: col@ing.univaq.it

A number of recent papers devoted to experimental investigation on masonry-infilled reinforced concrete (RC) frames under some strong lateral load, being their structure not conceived for that, can be mentioned. Al-Chaar et al. [1] studied five half-scale single-story specimens with a single, double, or triple bay, infilled by concrete or brick units, under monotonic loading. Mehrabi et al. [2] carried out monotonic and cyclic tests on twelve half-scale single-story single-bay specimens with concrete solid or hollow block infills, some of them being designed against wind pressure only. Buonopane and White [3] performed pseudo-dynamic (PD) tests on a single half-scale two-story two-bay specimen infilled with concrete hollow units. Pinto et al. [4] performed PD tests as well on two full-scale four-story three-bay specimens, bare and infilled with horizontally perforated bricks, respectively; then they repeated PD testing with retrofitted specimens. The two works mentioned last deal with infills that include openings. Lee and Woo [5] investigated performance of an one-fifth-scale two-bay three-story specimen, subjected to a series of earthquake-simulation shaking-table tests, and finally a pushover test.

Following previous experimental and numerical study dealing with infilled RC frames with their structures provided with a significant lateral strength [6, 7], a series of similar laboratory tests on seven single-bay single-story half-scale specimens have been carried out. Their frames are now characterized by columns being designed for gravity load only. Infills consist of non-reinforced masonry made of horizontally perforated brick and cement mortar. They are constructed in contact with the frames, but without any structural connection to them, as it is very usual in Italy and Mediterranean area. Seismic behavior is assessed by in-plane PD testing. Specimens differ with regard to: a) presence of infills, as two frames are tested bare; b) class of the frame reinforcement, as deformed and (weaker) round bars are alternatively used; lastly, c) aspect ratio, as two (infilled) specimens are not so squat as the others are. Infill openings are not covered.

Basic properties of both structural and non-structural materials, as derived from routine qualification test, are provided. Overall aspects of the seismic response are presented in some detail, in view of future model calibration and validation up to the member-by-member level. Local deformation in the frame is also analyzed, that might be useful for supporting more refined analysis models. The effect infills have at both the global and local level is stressed wherever it appears.

INFILLED FRAME SPECIMENS

Seven infilled RC frame specimens were constructed and tested. Their structures are drawn in Figure 1. The specimens marked U11 and U21 have an higher aspect ratio with respect to the specimens named V. The U11 and V1 specimens, plotted on the left-hand side, are reinforced by a round bar, the others by a stronger deformed bar. The V10 and V20 specimens are tested bare, the others infilled.

All specimens are intended to represent the lowest floor of a four-story building. The gravity load associated with upper stories is treated as vertical forces acting on the beam-column joints. It amounts to 190 kN per column for the U specimens, and 250 kN per column for the V specimens having a greater span. Compared to the concrete compressive average capacity, these loads are between 10% and 20%. It is important to notice that a single horizontal seismic force is assumed to be localized in the center of the beam. Thus the horizontal, PD seismic displacement is imposed there, where additional reinforcement has been placed.

Unfortunately, the beam-column joint cannot be said to represent that of an actual frame. In fact, the mere resultant of axial force in the upper column is applied on the upper face of the joint, and confinement by orthogonal beams is missing. Thus it was decided to preclude a possible (unrealistic) joint failure, by adopting a close spacing of the stirrups there, and to focus on the member behavior. Both beam and column longitudinal bars are anchored around the joint core by a single bent.

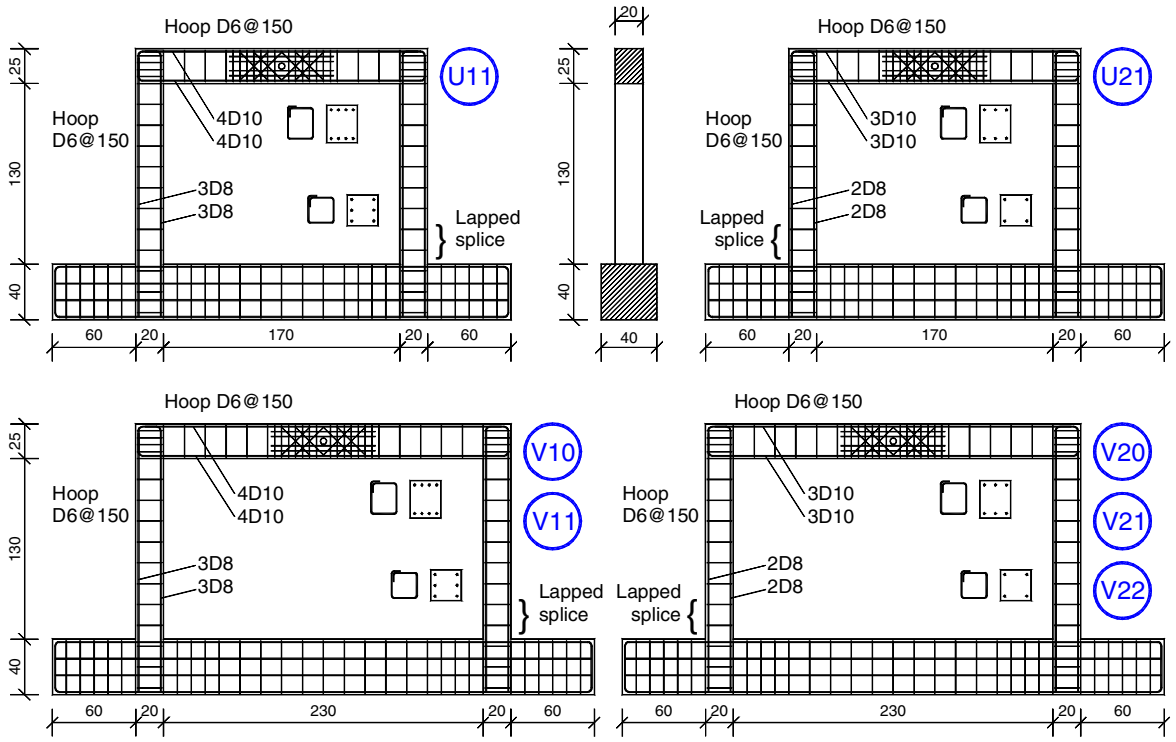

Figure 1. RC frame specimens (dimension unit is centimeter).

Column reinforcement is dictated by Italian non-seismic code provisions on its minimum quantity. In order to carry out some comparison, beam reinforcement is analogous to that designed for certain earthquake-resistant specimens tested previously, thus it is to some extent excessive for gravity load only. However, based on a moment-curvature fiber analysis of the member cross-section with average strength of materials, column bending moments at yield under gravity load result to be on average similar to those pertaining to the corresponding beam under pure flexure, while column bending moments at maximum strength are less than those pertaining to the beam. This is illustrated in Figure 2.

Figure 3 shows the frame horizontal strength consistent with two plastic mechanisms whose hinge reacting moments respectively are the yield bending moments and the maximum bending moments mentioned earlier. The frame strength associated with a shear failure of its members is plotted as well. Shear strength is evaluated according to Eurocode [8, Section 6.2.3], thus a lower and upper limit is foreseen, depending on the strut angle of inclination. All strengths are normalized by weight. As transverse reinforcement is low in any case, it seems flexure strength would govern failure.

Compressive strength and modulus of the frame concrete is reported in Table 1. Tension strength of the reinforcing steel, differentiated for each nominal diameter of the bar, is listed in Table 2. With respect to the deformed bars, classified as FeB44k in Italy, round bars used for the U11 and V1 specimens are weaker as they belong to a different, lower steel class named FeB32k. Lastly, Table 3 reports infill properties, as measured by vertical, horizontal, and diagonal compression tests performed on small-size walls. Cement mortar and horizontally perforated bricks, whose average dimensions are 77×246×242 mm, and void ratio equals 64.5%, are used to construct the infill masonry. Two unconnected panels 80 mm thick each (i.e., the nominal thickness of bricks) are built. Mortar is spread forming both head and bed joints approximately 10 mm thick, while the infill surface is not plastered for rendering.

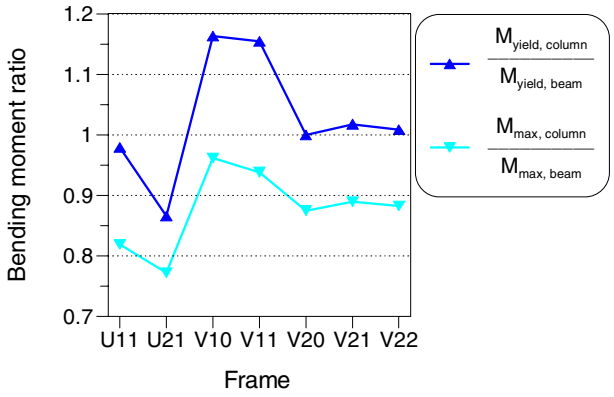

Figure 2. Member flexural strength.

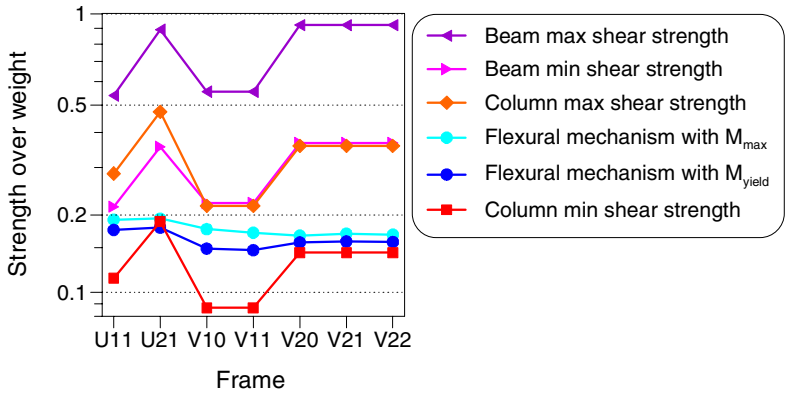

Figure 3. Frame flexural and shear strength.

Table 1. Average properties of concrete cylinder.

Frame		U11	U21	V10	V11	V20	V21	V22
Compressive strength	(MPa)	35.6	41.3	49.0	39.6	38.4	42.5	41.7
Elastic modulus*	(GPa)	33.2	35.5	35.3	33.1	32.4	30.1	31.7

*secant from 1/30th to 1/3rd of maximum strength (Italian UNI 6556 provision)

Table 2. Average strength of steel reinforcement.

Frame, Italian steel class		U11 & V1, FeB32k round			U21 & V2, FeB44k deformed		
Bar nominal diameter		D6	D8	D10	D6	D8	D10
Yield strength	(MPa)	345	385	364	572	558	553
Maximum strength	(MPa)	437	482	462	641	623	650

Table 3. Average properties of infill masonry.

	Vertical strength*	Horizontal strength*	Shear strength*	Vertical modulus**	Horizontal modulus**	Shear modulus**
(MPa)	2.24	2.56	0.35	—	3188	1574

*referring to gross area **referring to gross area and secant to maximum strength

LABORATORY EXPERIMENTS

The testing program that has been brought to a conclusion comprises the following several tasks: a) both structural and non-structural material characterization by routine tests on concrete cylinder, steel bar, infill brick, mortar prism, and small-size wall; b) measurement of stiffness and damping of bare and infilled frames in the linear elastic stage by (very) small-amplitude quasi-static cyclic and PD free-vibration tests; c) assessment of the inelastic seismic behavior of the specimens by their PD testing under a registered accelerogram at its natural intensity, being the specimens initially virgin, apart from occasional cracking of concrete and infill mortar due to their shrinkage; d) repetition of this same PD seismic test on the specimens damaged to that extent caused by the previous experiment; e) attainment to complete failure of the frames, made all bare, under quasi-static cyclic tests with an increasing displacement amplitude, carried out by imposing groups of three cycles whose amplitude equals one, two, and (where attained) three and four times the apparent yield displacement of the damaged frames.

With regard to the seismic PD tests, the infilled frame specimens are modeled as SDoF systems under an earthquake acceleration at their base. The explicit algorithm proposed by Shing and Mahin is used in order to numerically integrate the equation of motion [6]. Neither viscous nor numerical damping is introduced there, as some dissipation, amounting to a proper equivalent viscous damping ratio, is found to be naturally present in the experimental load-displacement loop. PD testing is carried out step-wise by using an electric endless-screw jack as the displacement actuator. In addition to those instruments that are indispensable to PD testing, passive supplemental instruments are placed, among which a number of inductive and potentiometer displacement transducers for deriving deformation in the potential critical regions at the member ends.

Quantities are scaled to the specimen level by similitude laws. Being length reduced to half size, and assuming the story mass to be preponderant, time must contract by $\sqrt{2}/2$. This is fulfilled with the use of a shrunk accelerogram in the numerical integration. In the followings, results are conveniently presented in terms of specimen's scaled quantities, except for time, which is converted to the prototype level.

The accelerogram selected for PD seismic testing is the east-west record from Tolmezzo (Friuli, Italy) earthquake dated May 6th 1976. Its peak value equals 32% of the gravity acceleration. A significant portion only of this accelerogram is considered, as shown in Figure 4. Its corresponding 5% damped normalized elastic response spectrum of the absolute acceleration and relative velocity as well is plotted in Figure 5, together with some additional data to be commented later on.

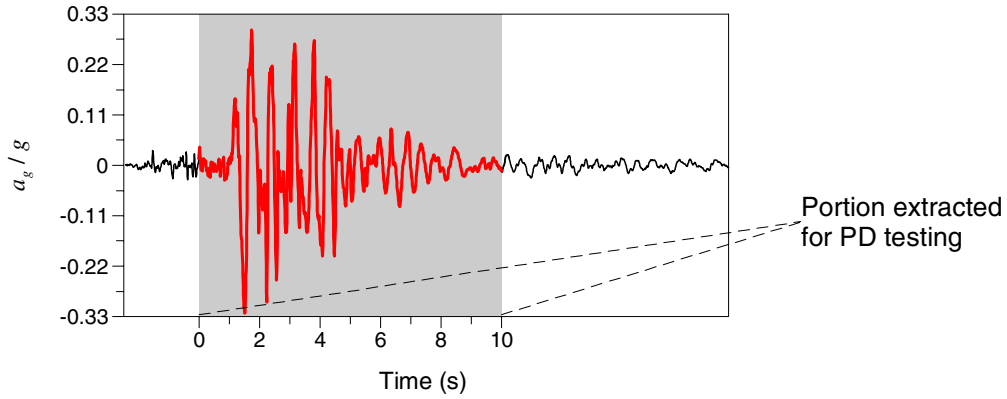

Figure 4. Tolmezzo (Friuli, Italy) accelerogram.

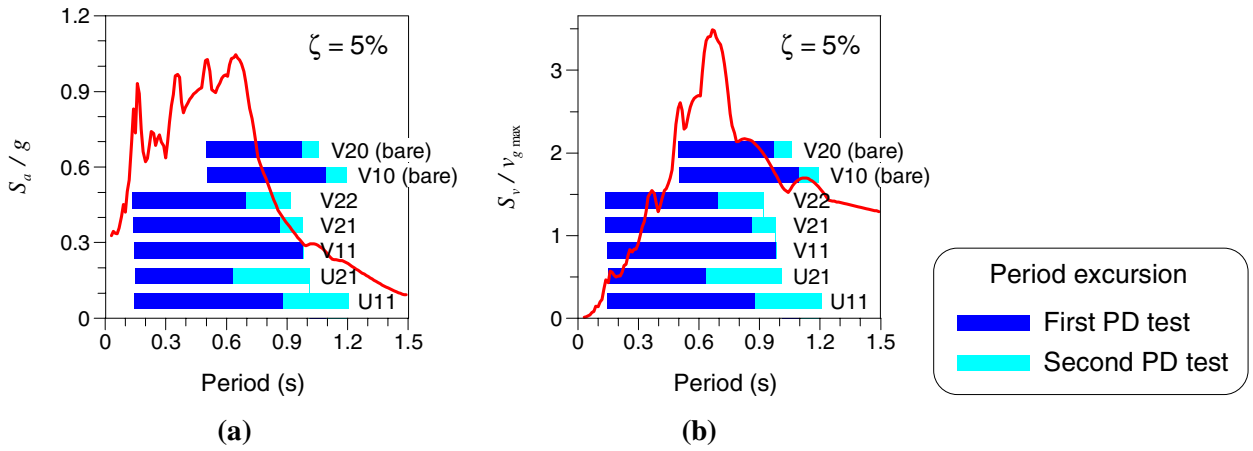

Figure 5. (a) Acceleration and (b) velocity response spectrum of the selected accelerogram.

As the infilled frame specimens are thought to represent the lowest floor of a four-story building, the mass pertaining to all upper stories is introduced into the equation of motion to be integrated during both free-vibration and seismic PD tests. Its corresponding gravity load, specified earlier, is held over the beam-column joints by two hydraulic jacks pushing against an articulated steel frame, which is able to follow the horizontal displacement of the specimen. This gravity load is adjusted by manual control throughout every experiment, pseudo-dynamic and cyclic as well.

It is well-known that experimental errors, those of a systematic nature in particular, may be so detrimental to PD tests that numerical integration may even diverge, especially where stiff specimens are of concern. Accuracy of the performed tests has been analyzed elsewhere, and found to be satisfactory [9].

PD TEST RESULTS

Damage description

Owing to the first PD test, in the frames cracks early appeared localized in the beam ends, and some of them extended over the full depth of the cross-section. Column cracks spread along the height on that face being not in contact with the infill, and opened to a lesser extent, so much so that most of them closed as the rest position was gained. Longitudinal cracking was occasionally seen in association with lapped splices. Two additional, specific features were observed. Firstly, cracks inclined at one or both column tops in the only frames with a deformed bar. Secondly, concrete generally began to crumble, this systematically exposing the hoops in all and only those beams with a round bar instead. Longitudinal reinforcement was slightly disclosed in one column bottom only of the bare V20 specimen.

Besides emphasizing what has been just described, the repeated PD test caused visible bar buckling to affect some U and V members as well. Various conditions can be appreciated by photos in Figure 6. Relatively severe damage occurring in the U11 beam is seen in Figure 6a. The most outstanding case of bar buckling in combination with inclined cracking in the column top is illustrated in Figure 6b. Figure 6c shows an example of column cracking and crushing in the lowest half. Concrete crushing was the most clearly noted at the column bottom of those frames tested bare, as in Figure 6d. In addition, slippage from the beam-column joint of longitudinal reinforcement placed in the beam was noticed in those specimens where a round bar was used, so much so that outward pushing of the bar bent caused the concrete cover of the joint to crack, and somewhere to break off.

(a) **(b)** **(c)** **(d)**

Figure 6. Frame damage in the end of the second PD test; cracks in (c) have been marked.

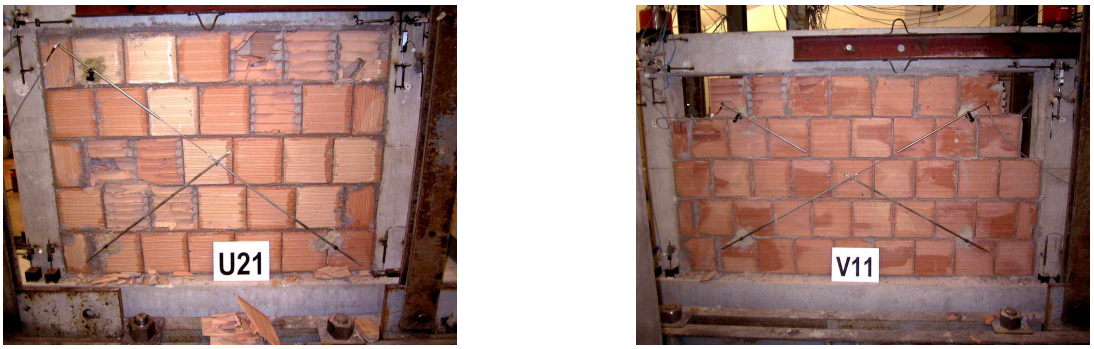

(a) **(b)**

Figure 7. Infill damage in the end of the first PD test.

Infills exhibited severe damage already in the course of the first PD test. Cracking indifferently affected brick and mortar joint, and failure consisted in masonry crushing. This tended to occur in the center of the infills with an higher aspect ratio (Figure 7a), whilst it clearly localized at the corners of the squat infills (Figure 7b). Due to the stiff foundation beam, supposed to be in contact with the infill along a greater length with respect to the top beam, corner crushing was specific to upper corners (Figure 7b).

Stiffness

Various stiffness measures are reported in Table 4. These in listing order are: the tangent, initial stiffness of the bare and infilled specimens in the absence of any seismic damage, where such measure was taken; the tangent stiffness after first cracking of the infill or the frame, for the infilled or bare specimens respectively, that was generally identified both at sight and as stiffness appeared to decrease in the load-displacement curve; lastly, the tangent stiffness beyond pinching, if any, in the end of each PD test.

It is noticed the effect of infills initially is dramatic, as the frame once infilled results to be one order of magnitude stiffer than when bare. The U specimens, having an higher aspect ratio, exhibit a smaller initial stiffness, as one would expect. However, merely due to first cracking of the infill, stiffness to a great extent decreases, much more than what pertains to the bare V10 and V20 frames. In the end of PD testing, in association with the damage scenario described earlier, difference between the stiffness of the infilled and bare specimens almost vanishes. The V10 and V20 frames, tested bare, there clearly exhibit a greater stiffness, as a percentage of its initial value, than the infilled specimens do.

Table 4. Stiffness of the specimens (italic denotes bare frames).

Specimen		U11	U21	V11	V21	V22	V10	V20
Initial of bare frame	(kN mm^{-1})	—	—	*18.5*	*18.8*	—	*15.4*	*15.9*
Initial of infilled frame	(kN mm^{-1})	141.9	132.5	186.3	210.1	206.4	—	—
After first cracking of infill/frame	(kN mm^{-1})	50.0	21.6	29.2	26.7	39.5	*6.5*	*4.5*
In the end of first PD test	(kN mm^{-1})	3.9	7.5	4.1	5.3	8.2	*3.3*	*4.2*
In the end of second PD test	(kN mm^{-1})	2.1	3.0	4.0	4.1	4.7	*2.8*	*3.5*

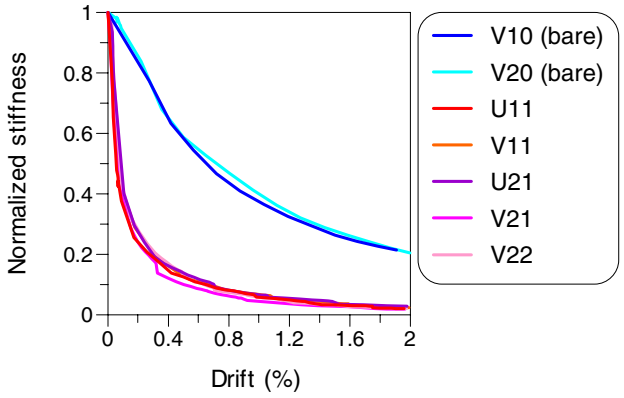

Figure 8. Stiffness secant to load-displacement envelope.

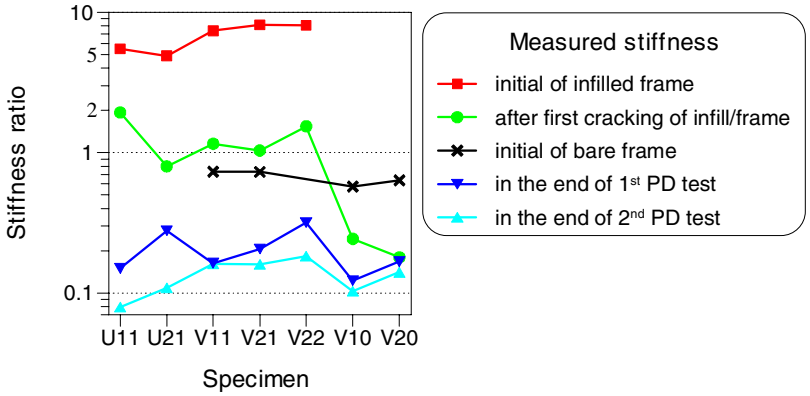

Figure 9. Measured stiffness over virgin bare frame theoretical stiffness.

Deterioration of infilled specimens' stiffness is confirmed to be marked, and early as well, by examining Figure 8. Stiffness secant to the load-displacement envelope of both PD tests is there plotted versus story drift. This secant stiffness is normalized by the initial stiffness of each corresponding specimen, infilled or bare. Substantial agreement is observed among infilled specimens, and between the two bare frames as well. How much pronounced stiffness decrease is in the case of infilled specimens clearly appears. It follows a significant period elongation is expected. This can be appreciated in Figure 5, where period excursions as derived from tangent stiffness are illustrated. As a matter of fact, with respect to the selected accelerogram infills make the specimens exposed to the whole range of the peak spectral ordinates.

It is worth to compare measured stiffness listed in Table 4 with the theoretical stiffness of a virgin bare frame with fixed-end column and concrete gross section, being the concrete elastic modulus predicted on the basis of its compressive strength according to Eurocode [8, Section 3.1.3]. The ratio of the former (measured) stiffness divided by the latter (theoretical) one is plotted in Figure 9. Virgin bare specimen's measured stiffness is 57% to 73% of the theoretical one, as the middle curve shows. Measured stiffness of the virgin infilled specimen is 5 to 8 times the theoretical stiffness of the virgin bare frame. Measured stiffness of the infilled specimens after infill cracking however is greater than the theoretical stiffness of the virgin bare frame, up to 1.9 times, with the exception of the U21 specimen. In turn, measured stiffness of the bare specimen after frame cracking is around 20% of the theoretical one. A similar ratio is found for the infilled specimens in the end of the first PD test.

Strength and displacement

The most important measures of load, and story drift as well, registered during each PD test, are collected in Table 5. These are the first cracking load and related drift (again, cracking refers to infill for the infilled specimen, or concrete for the bare one), the maximum load and related drift, and the maximum drift, all of them in absolute value. For the sake of completeness, the same measures pertinent to the final cyclic test, performed with damaged specimens made all bare, are also reported in Table 5.

Measured maximum loads are plotted in Figure 10 normalized by the plastic mechanism strength of the bare frames, being yield bending moments derived from a moment-curvature fiber analysis of the member cross-section with average strength of materials. In order to evaluate this estimated strength, the normalized maximum load measured in the final cyclic test with the bare (damaged) frames is plotted in Figure 10 as well. Ratios in the range 0.86 to 1.09 are seen, that may be said reasonable if one invokes cyclic deterioration or, conversely, steel hardening. The frame minimum strength associated with column shear failure according to Eurocode [8, Section 6.2.3] is also scaled and plotted in Figure 10.

Referring to infilled specimens in the first PD test, in Table 5 one notices that, similarly to stiffness, an higher aspect ratio is associated with a their smaller cracking load, and maximum load as well. Primarily, the results show that maximum strength is to a considerable extent greater compared to that of bare specimens. It can be appreciated in Figure 10 that the infilled specimen strength ratio is 2.2 to 2.8 in the first PD test. Coming to damaged specimens in the second PD test, this same ratio noticeably lessens, nevertheless it clearly remains higher with respect to that concerning bare frames. Therefore infills, though damaged as previously described, significantly contribute to maximum strength still. The V10 and V20 specimens, tested bare in every test, are seen to exhibit almost the same ratio in any experiment, apart from a little strength decrease passing from the first PD test to the second one.

Table 5. Strength and drift of the specimens (italic denotes bare frames).

Specimen			U11	U21	V11	V21	V22	V10	V20
1st PD test	Cracking load	(kN)	50	40	55	80	85	*20*	*25*
	Maximum load	(kN)	155	159	190	175	221	*80*	*98*
	Cracking drift	(‰)	0.25	0.19	0.22	0.26	0.28	*1.13*	*1.16*
	Drift at maximum load	(%)	0.83	0.70	1.10	0.32	0.62	*2.02*	*1.58*
	Maximum drift	(%)	1.75	1.49	2.21	2.06	1.52	*2.46*	*2.54*
2nd PD test	Maximum load	(kN)	98	131	101	120	143	*67*	*86*
	Drift al maximum load	(%)	2.23	1.87	2.04	2.12	1.51	*1.43*	*2.35*
	Maximum drift	(%)	2.24	2.41	2.18	2.15	2.26	*2.48*	*2.41*
Final ciclic test	Maximum load	(kN)	*57*	*74*	*65*	*77*	*86*	*65*	*84*
	Drift al maximum load	(%)	*2.46*	*2.21*	*2.46*	*2.46*	*2.39*	*2.46*	*3.54*
	Maximum drift	(%)	*7.37*	*7.37*	*7.37*	*2.46*	*4.91*	*7.37*	*4.91*

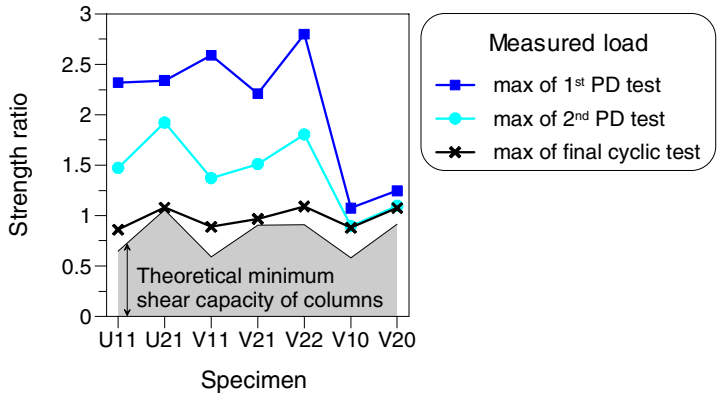

Figure 10. Measured load over flexural plastic mechanism strength of bare frame.

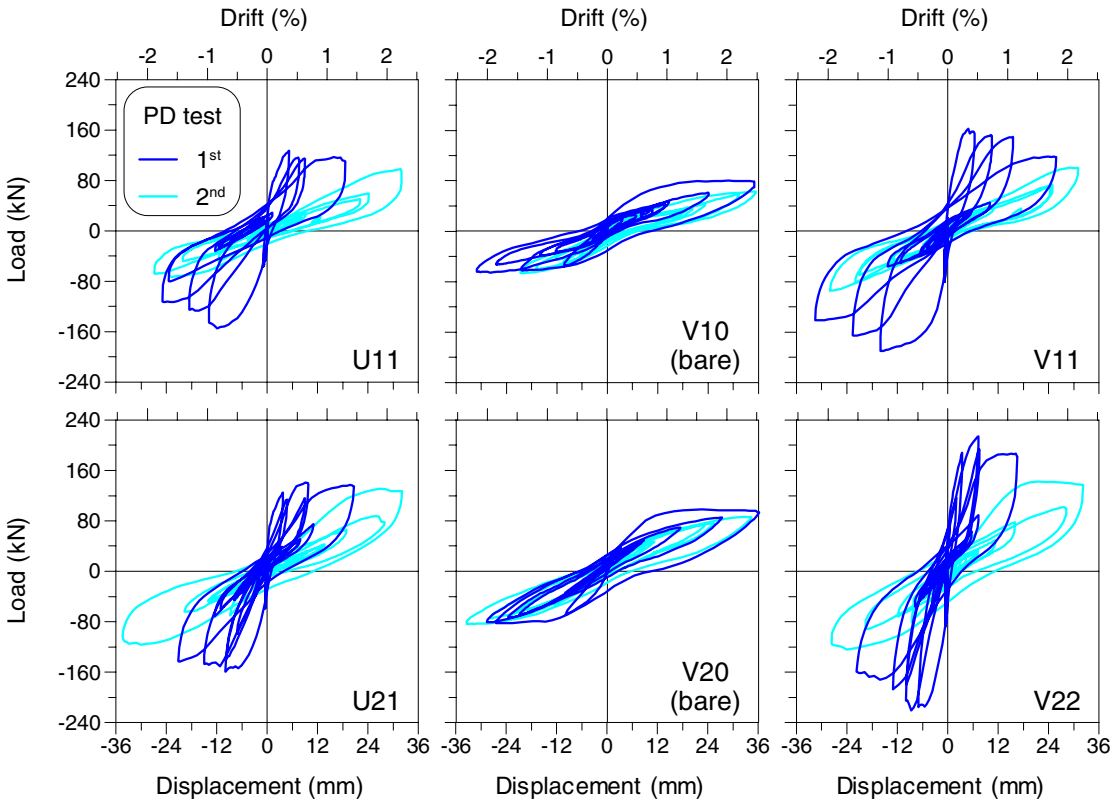

Figure 11. Load-displacement curve of PD tests.

Load-displacement curves of all but the V21 specimen in both PD tests are illustrated in Figure 11. Anew, the effect of infills in terms of increased maximum strength is clearly seen as being prominent. Strength deterioration as cycling proceeds is apparent as well. It follows that difference between loops pertaining to the bare and infilled V specimens evidently reduces in the second PD test. Going into details, there it seems some additional dissipation capacity can be exploited by infilled specimens, as the bare ones exhibit a sharper loop, in spite of a their greater peak displacement.

As regards displacement, a quite small drift at first cracking of the infill, amounting to less than 0.3‰, is found in Table 5. Contrarily to initial stiffness, and both cracking and maximum load, this drift does not show any clear correlation with specimens' aspect ratio. Drift at maximum strength and maximum drift as well, compared in the case of infilled versus bare specimens, to a greater extent vary in the first PD test than they do in the second one, as depicted in Figure 12. Drift at maximum strength in the second PD test traces that in the final cyclic test with bare specimens. All this confirms deterioration is of concern.

Peak values apart, displacement in its details deserves a comment. Displacement time histories are plotted in Figure 13, which refers to both PD tests, on the left-hand and right-hand side, respectively. Starting with the first experiment, the bare V10 and V20 specimens are seen to undergo their peak displacement quite early, before two seconds of response (and this prevents cyclic strength deterioration from being emphasized, Figure 11). Contrarily, the infilled specimens do so near four seconds of their response, after an oscillation of increasing amplitude. This seems reasonable by the light of stiffness decrease, and consequent period elongation, compared to response spectra (Figure 5). Coming to the second PD test, on the right-hand side of Figure 13, difference among infilled and bare specimens disappear. As a matter of fact, every time history is now characterized by attaining the peak displacement early. Displacement there seems to be not so strongly affected by damaged infills as maximum strength is.

It is worth also to notice the difference existing between the nominally identical V21 and V22 specimens in the first PD test, whereas a their substantial agreement results in the second one. This is consistent with the fact that their stiffness after infill cracking (Table 4), and maximum strength as well (Table 5), is quite dissimilar. On the basis of numeric simulation, analogous results have been explained by scattering of the infill properties [7]. In addition, as the present infills consist of two walls, different contact conditions, e.g. due to workmanship or mortar shrinkage, may yield their responses to be not perfectly parallel.

Energy

As various energies, absolute and relative as well [10], are calculated, the time history of absolute input energy is found to resemble that of relative input energy. Major increments appear in connection with the oscillations of a greater amplitude, that is they occur more and more during the first PD test on infilled specimens, whilst in the early stage of the response of the bare and damaged infilled specimens. Maximum values of absolute and relative input energy result to be essentially similar. Their difference is around 5% or less, as expected where natural periods match those of the ground motion [10]. Maximum values are indifferently found during the response or in the end of the accelerogram, where computation is stopped. Maximum absolute (relative) input energy at most is 6% (8%) greater than its final value.

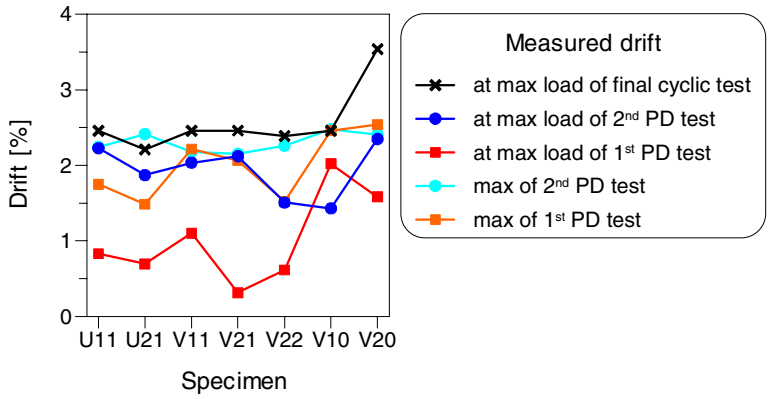

Figure 12. Measured drift.

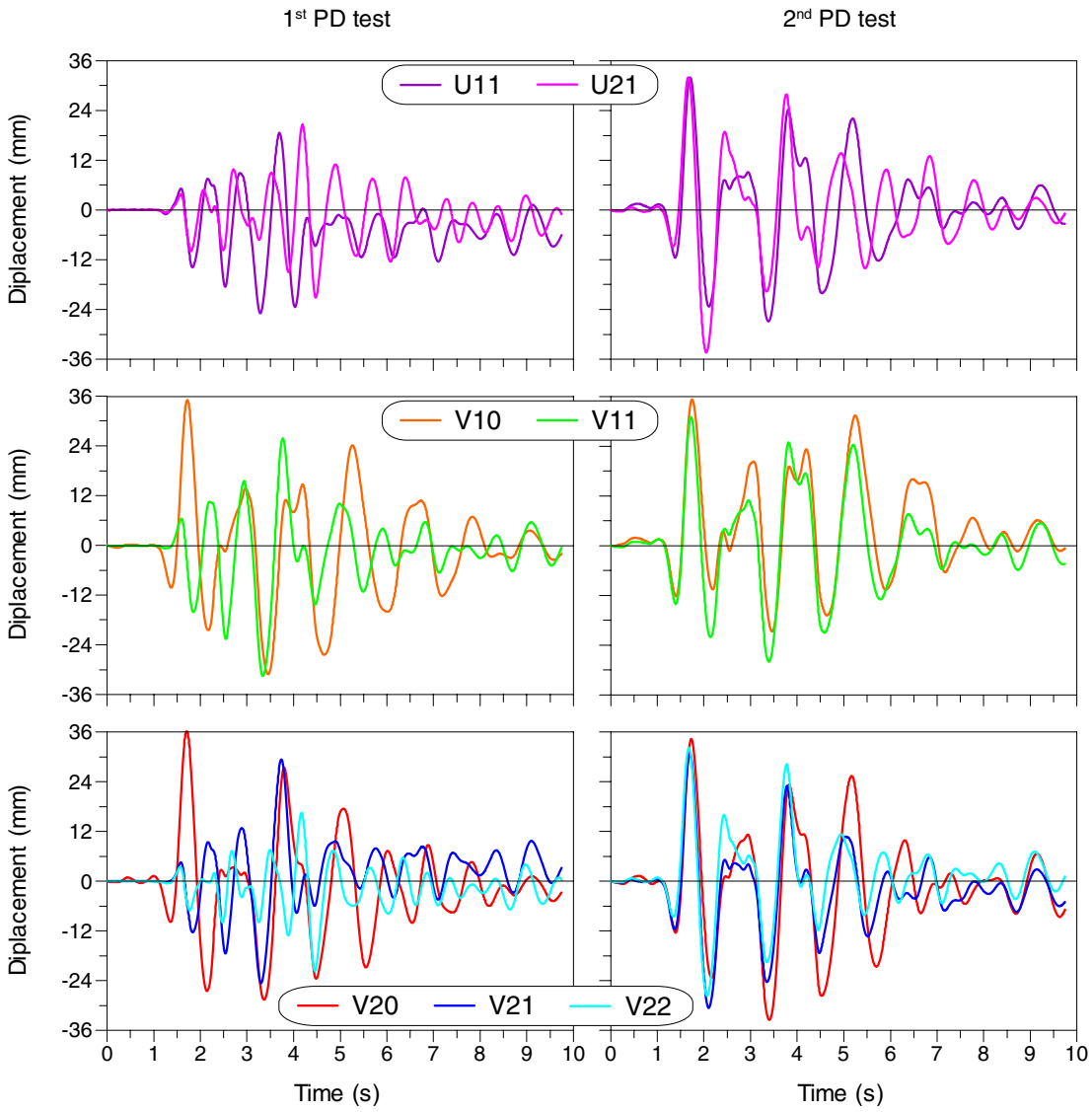

Figure 13. Displacement time history of PD tests.

As viscous damping energy is not present, and kinetic energies almost vanish in the end of both PD tests, absorbed energy finally attains about the same value as input energy, absolute and relative as well. Furthermore, oscillation in the time history of absorbed energy, associated with strain energy, is found to become rather little eventually. Thus final absorbed energy can approximately be regarded as final input energy, and hysteresis dissipated energy as well.

Final values of absorbed energy in each PD test are plotted in Figure 14 (see the top two curves). Normalization by the kinetic energy associated with the peak ground velocity is assumed (recall that specimens' mass is different). As far as the first PD test is concerned, absorbed (and, approximately, input, and hysteresis) energy per unit of mass is similar among infilled specimens, and clearly greater than that pertinent to the bare V10 and V20 specimens. In the second PD test energy decreases, and a greater difference is seen among the infilled specimens. It is interesting to notice that period excursion in Figure 5 tends to be wider for those specimens experiencing a smaller energy demand in the second PD test.

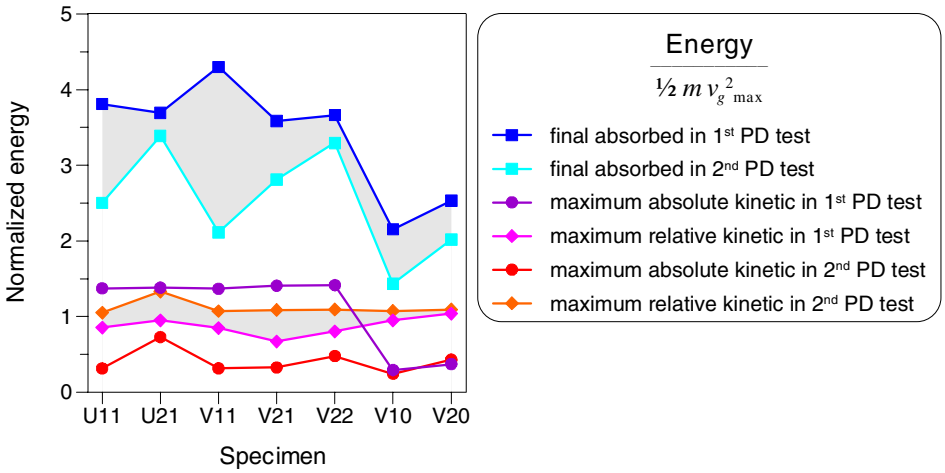

Figure 14. Normalized absorbed and kinetic energy.

Maximum values of normalized absolute and relative kinetic energy in both PD tests are also plotted in Figure 14. It is seen that in the first test absolute kinetic energy is greater than relative kinetic energy, but for the V10 and V20 specimens tested bare. Relative kinetic energy however prevails in the second test with damaged specimens. Such a result is what one would expect thinking about an extremely stiff system, that essentially moves as the ground does, opposed to an extremely flexible system, whose absolute velocity is almost null. Thus different periods of the infilled frames in the virgin or damaged state reflect on their absolute and relative kinetic energy, rather than on input energy.

One would ask to what extent infills, being responsible for stiffening and a greater energy demand, contribute to energy dissipation; in other words, whether frames are relieved or not with respect to the case they were bare. Unfortunately, the final cyclic test carried out with bare specimens do not show any systematic result in this sense. Some frames previously tested infilled exhibit a greater residual capacity with respect to a similar frame previously tested bare, whilst other frames do not.

Local deformation in the frame

Besides importantly affecting overall properties and response, infills are also found to govern the local, inelastic deformation in the frame. In essence, local deformation is led to be localized and asymmetric. Extreme rotation of member ends apart, listed in Table 6, this is best appreciated by examining measures at a same instant of the response. Selected results are illustrated in Figure 15 referring to two distinct conditions. The first one corresponds to the first peak drift beyond 5‰, that approximately is where maximum strength was exploited by infilled specimens. The other condition is at the maximum drift during the second PD test, i.e. after significant cycling, and accumulation of plastic deformation, and infill damage, has occurred. In order to make deformation comparable among various specimens under a their different drift, deformation is normalized by the drift itself (expressed in radian for the rotation).

As regards infilled specimens, deformation clearly appears to concentrate in the windward end of the beam, while it remains negligible in its leeward end. In effect, one should consider that as the horizontal displacement is applied to the center of the beam, its axial force is compression in one half, and tension in the other. The infill, behaving in analogy with a bracing diagonal strut, stresses tension in the windward end of the beam, whose yield bending moment decreases. Rotation with frame's inner fibers elongated, assumed to be positive, is evidently greater than the opposite rotation in the case of infilled specimens (Table 6). This effect remains in the second PD test, despite infills are to a great extent damaged.

Table 6. Rotation of the member ends (unit: radian×10^{-3}; italic denotes bare frames).

Specimen			U11	U21	V11	V21	V22	V10	V20
1st PD test	Beam end	max	26.8	15.2	46.4	16.0	20.0	*17.6*	*14.8*
		min	-1.4	-1.4	-7.5	-2.7	-1.9	*-12.3*	*-8.6*
	Column top	max	8.8	11.1	2.5	6.8	1.3	*5.1*	*6.5*
		min	-7.7	-5.5	-5.9	-18.8	-7.1	*-16.9*	*-12.7*
	Column bottom	max	14.5	14.8	20.6	20.1	12.2	*22.1*	*28.7*
		min	-8.3	-6.2	-4.1	-5.0	-2.4	*-20.6*	*-15.6*
2nd PD test	Beam end	max	31.4	21.4	37.2	16.6	25.5	*22.6*	*18.3*
		min	-4.5	-0.9	-15.9	0.2	-5.1	*-16.6*	*-10.4*
	Column top	max	9.9	8.6	0.4	5.9	1.7	*-0.4*	*5.9*
		min	-11.7	-19.8	-5.1	-26.9	-14.4	*-13.0*	*-11.6*
	Column bottom	max	18.4	23.4	20.6	24.3	21.0	*16.8*	*34.7*
		min	-12.3	-10.9	-5.1	-7.4	-8.6	*-19.8*	*-19.5*

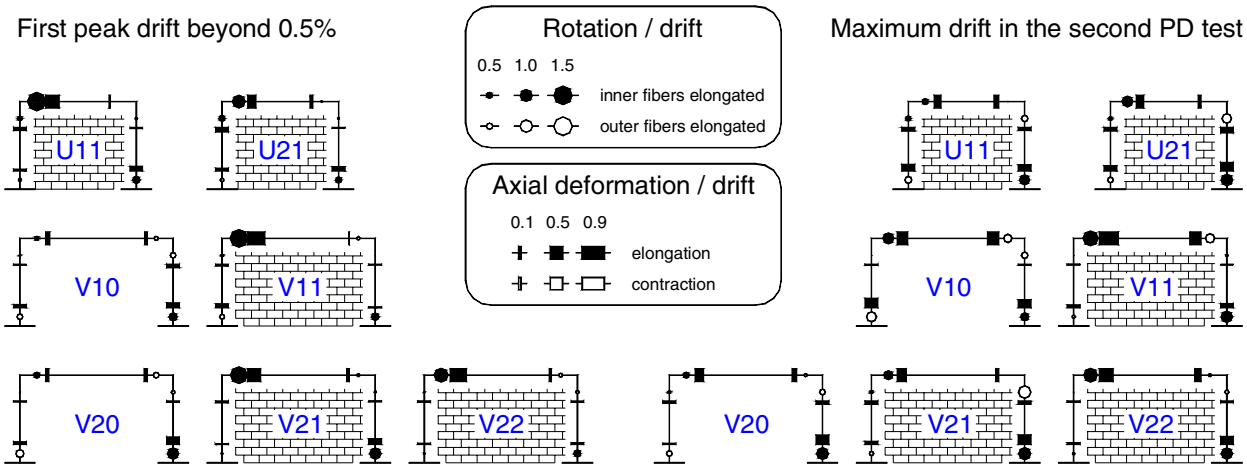

Figure 15. Normalized deformation of the member ends (story sway is towards right).

Smallest deformation is noticed in the windward column of the infilled frames. In fact, when a column is in the windward stage, rotation of its base is precluded by the infill (which sustained little damage in the bottom corners, as previously described). Contrarily, significant rotation takes place there in the leeward stage, as the column comes off the infill and freely inflects along its height. Referring to the column top, important rotation is occasionally seen in the leeward stage as well. However, it should be considered that in those cases where upper corners of the infill crushed, rotation has to be expected somewhere along the windward column, while it was not measured there. The corresponding upper rotation seems to be located in the beam end, made to some extent weaker by tension, rather than in the column top.

CONCLUSIONS

Seismic behavior of infilled RC specimens with their structure designed for gravity load has been studied by in-plane PD testing. Infills consisting of cement mortar and perforated bricks are of concern. Even though their void percent is relatively great, typical results are confirmed, in that infills are found to substantially influence basic properties. In fact, the initial stiffness increases by approximately one order of magnitude with respect to the bare frame, while maximum strength doubles and more. However, as

seismic cycling proceeds, deterioration of such properties is apparent. Stiffness deterioration is more marked than strength deterioration is.

Consequently, the overall seismic response of infilled specimens considerably differs from that of bare frames, in its features if not in peak quantities. This to a lesser extent holds among infilled specimens themselves, it seems due to scattering of infill properties. On the contrary, substantial similitude is noticed where the response of damaged specimens, both infilled and bare, is considered.

Energy analysis shows that infilled frames are prone to a greater input, and absorbed, energy. Anew, this statement has to be to some extent relaxed in the presence of damage. A greater energy demand does not necessarily imply a greater supply by the frame, as the infill contributes to dissipation. Rather than stiffening, the most important negative effect of infills, being related to the way the seismic load acts, consists in altering the internal stress distribution in the frame. This causes its plastic deformation to be asymmetric and, mostly, localized.

Possibility of such redistribution should be taken into account in the assessment of existing buildings, at least by means of simplified models like equivalent diagonal struts hinged somewhere along columns. Otherwise, it is believed it would be not conservative to rely on infills for strength and dissipation capacity at the global level, and nothing more. Besides uncertainty on basic properties, and their early deterioration where significant cyclic ductility is of concern, a local structural failure may occur.

ACKNOWLEDGEMENTS

The PD system was partly funded by Italian Ministry of University, and of Scientific and Technological Research. The National Research Council of Italy, GNDT Group, financed the tested specimens.

REFERENCES

1. Al-Chaar G, Issa M, Sweeney S. “Behavior of masonry-infilled nonductile reinforced concrete frames.” Journal of Structural Engineering 2002; 128(8): 1055-63.
2. Mehrabi AB, Shing PB, Schuller MP, Noland JL. “Experimental evaluation of masonry-infilled RC frames.” Journal of Structural Engineering 1996; 122(3): 228-37.
3. Buonopane SG, White RN. “Pseudodynamic testing of masonry infilled reinforced concrete frame.” Journal of Structural Engineering 1999; 125(6): 578-89.
4. Pinto A, Varum H, Molina J. “Experimental assessment and retrofit of full-scale models of existing RC frames.” Proceedings of the 12th European Conference on Earthquake Engineering, London, UK. Paper no. 855. Amsterdam: Elsevier, 2002.
5. Lee H-S, Woo S-W. “Effect of masonry infills on seismic performance of a 3-storey RC frame with non-seismic detailing.” Earthquake Engineering and Structural Dynamics 2002; 31: 353-78.
6. Colangelo F. “Pseudodynamic tests on brick-infilled RC frames.” Proceedings of the 11th World Conf. on Earthquake Engineering, Acapulco, Mexico. Paper no. 1360. Oxford: Pergamon, 1996.
7. Colangelo F. “Experimental evaluation of member-by-member models and damage indices for infilled frames.” Journal of Earthquake Engineering 2003; 7(1): 25-50.
8. CEN Technical Committee 250. “Eurocode 2—General rules and rules for buildings.” prEN 1992-1. Brussels: CEN, 2001.
9. Colangelo F. “Overshooting error in inelastic pseudodynamic tests on stiff specimens.” Proceedings of the Eleventh International Conf. on Computational Methods and Experimental Measurements, Halkidiki, Greece. Southampton: WITPress, 2003: 119-28.
10. Uang C-M, Bertero VV. “Evaluation of seismic energy in structures.” Earthquake Engineering and Structural Dynamics 1990; 19: 77-90.